Published in: 2017 IEEE 85th Vehicular Technology Conference (VTC Spring)
DOI: 10.1109/VTCSpring.2017.8108515

Rushing Full Speed with LTE-Advanced is Economical - A Power Consumption Analysis

Robert Falkenberg, Benjamin Sliwa and Christian Wietfeld
Communication Networks Institute
TU Dortmund University
44227 Dortmund, Germany
Email: {Robert.Falkenberg, Benjamin.Sliwa, Christian.Wietfeld}@tu-dortmund.de

***Abstract*—Boosting data rates in LTE mobile networks is one of the key features of LTE-Advanced. This improved user experience is achieved by Carrier Aggregation (CA), in which the available spectrum of an operator is bundled out of several frequency bands. Accordingly, the user equipment has to supply multiple reception chains and therefore consumes considerably more power during a transmission. On the other hand, transmissions terminate faster, which enables a quick switchover into energy-saving mode. In order to examine these opposed facts, empirical analyses of existing devices are first carried out. Subsequently, we present a new CA enhancement of an existing context-aware power consumption model which incorporates the development density of the environment and the mobile device mobility. Based on the extended model we perform a detailed power consumption analysis and show that CA leads to power savings of 31 % if the data rate doubled for large file transmissions. In addition, we show that CA can lead to power savings even from a data rate increase of 25 %, regardless of mobility and urban development density. Besides, the measurement results show that CA operated in the same band leads to a lower power consumption than inter-band CA.**

I. Introduction

The ongoing evolution of Long Term Evolution (LTE) mobile networks increases the achievable data rate over the radio link. A prominent example is the Carrier Aggregation (CA) feature of LTE-Advanced (LTE-A) networks in which, as shown in Fig. 1, the data is transmitted simultaneously over multiple distributed frequency bands possessed by a single network operator in order to boost the data rate of the connection. While data rates increased in the recent years, in spite of more and more efficient system-on-chips and new power-saving techniques, the battery lifetimes of mobile devices did not. This is caused by the growing demands on the provided content: the resolution of video streams increases, websites and documents contain more complex graphical components, and the amount of data which is being stored and processed by cloud services grows continually. As the lion share of today's smartphone traffic is issued in the downlink due to streaming and downloading web content, operators in Europe began to roll out LTE-A networks supporting CA in the downlink.

For an LTE-A modem the reception of multiple carriers requires powering a corresponding number of receive chains and additional signal processing. At this point arises the question how the power consumption of an LTE-A device is affected by CA. On the one hand, as illustrated in Fig. 1, CA leads to an increased power draw within the User Equipment (UE). On the other hand, the data rate is significantly boosted, hence allowing a faster termination of transmissions.

The objective of this work is to analyze the power consumption of today's LTE-A devices and to utilize this empirical knowledge for consumption simulations in numerous usage patterns, environments, and mobility scenarios, e.g. for a moving vehicle. This allows the identification of situations where CA reduces the power draw of UE and therefore increases the battery lifetime of mobile devices.

For this purpose, an established power consumption model will be extended for downlink CA in Sec. III. Afterwards, Sec. IV covers empirical measurements with existing LTE-A devices followed by various simulations in Sec. V which are based on the gained values and the proposed model extension. The paper closes with a brief summary and conclusion on the results.

II. Related Work

The power consumption of LTE equipment has been measured, modeled and analyzed in numerous studies. In [1] a power consumption model for downlink and uplink is presented based on empirical measurements. It shows that the power consumption for the uplink is mostly affected by the transmission power rather than by the uplink data rate. Complementary, the power draw invoked by downlink reception mostly depends on the data rate rather than received signal power. The most complex procedure in the reception process is the iterative turbo decoding whose complexity linearly scales with the data rate. This fact was confirmed in [2] as the downlink power consumption induced by the turbo decoder of

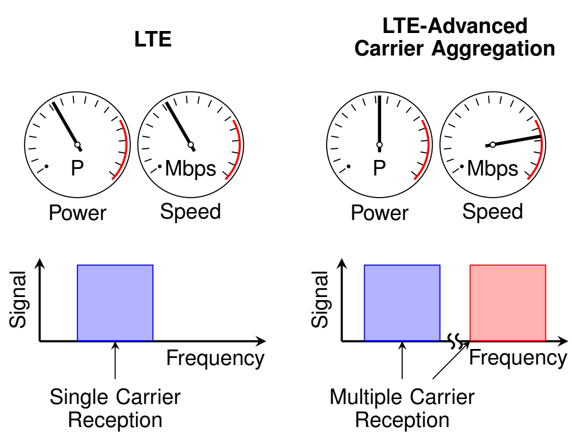

Fig. 1. Functional Principle of Carrier Aggregation and its Influence on Data Rate and Power Consumption

newer devices linearly grows by 5 % if the number of allocated Resource Blocks (RBs) increases by factor 10. In case of an LTE cell with multiple UEs claiming for a large number of radio resources (e.g., large file transfers) it is energy efficient to share the available RBs in time rather than in frequency [3]. By doing so, single UEs process larger chunks of data for a short time and save energy in the remaining period instead of powering the decoder continuously.

Moreover, the authors of [2] attend on the energy-efficiency evolution in the past few years. They point out a reduction of transmission-power consumption by 35 % at low and intermediate output power levels as well as for the entire reception process. Besides, the uplink power consumption of LTE UE is independent from the actual uplink data rate.

In [4] an empirical analysis of the current consumption of first-generation LTE-Advanced devices has been performed. The authors have measured power savings of 13 % by enabling CA for large File Transfer Protocol (FTP) downloads. The authors of [5] were able to confirm the same effect by their measurements. Due to restrictions of the Device Under Test (DUT) in both studies, no intra-band CA could be analyzed, so our measurements will close this gap.

Since laboratory measurements typically lack of generality and field measurements often cannot be performed in the required extent, a context aware power consumption model has been developed in [6] to perform representative simulations of the UE's power consumption. The model considers the radio channel (static, fading), environment (urban, rural), data size, arrival rate, UE power consumption in different operation modes, as well as further parameters. From these parameters the model calculates the average long-term power consumption of the UE. The development and evaluation of the model showed that the transmission of data in uplink direction is the most energy-intensive part of an LTE modem – especially at high transmission power.

Furthermore, the model has been extended for LTE-A uplink analysis [7] and analyzed in theory. To the best of our knowledge the model has not been adapted for an LTE-A downlink analysis, which will be proposed in this paper.

III. Power Consumption Model

Performing representative simulations on the impact of CA on the UE's power consumption requires an exact power model of the analyzed device as well as an incorporation of external influencing factors like the environment and mobility. For this reason the proposed power consumption model for downlink CA is based on the excessively studied Context-Aware Power Consumption Model (CoPoMo) presented in [6]. In order to facilitate a better understanding of the presented approach, an introduction to the underlying model is given in the next section. For full details the reader is kindly referred to the full documentation in [3] and [6].

A. Uplink Power Consumption Model

One central statement of CoPoMo is the outcome that the amount of power an LTE modem requires is highly depending on its transmission power and the time spent in this mode. The authors have reduced the complexity of uplink power consumption to four main power states (Idle, Low, High, Max)

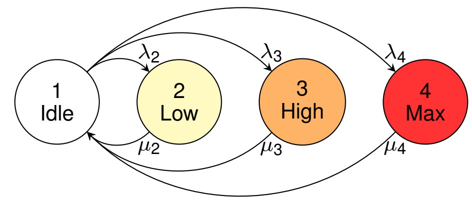

Fig. 2. Markovian Power State Model of LTE User Equipment

TABLE I
Properties of the Simulated Environments According to [6] if not Noted Otherwise

Environment	Inter Site Distance
Urban	500 m [8]
Suburban	1732 m [8]
Rural	5000 m
Channel model	**Mobility**
Additional White Gaussian Noise (AWGN)	0 km/h
Pedestrian	3 km/h
Vehicular	60 km/h
Frequency Band	**Bandwidth**
800 MHz (Band 20)	10 MHz
2600 MHz (Band 7)	10 MHz

a UE may enter according to the current radio conditions while still maintaining a very high model accuracy. Each state i is characterized by an average power consumption $\bar{P}_i$ obtained from empirical measurements of the actually analyzed device (cf. IV). Furthermore, downlink transmissions without any uplink component result in entering the Low power state regardless of the radio conditions. Those states, in conjunction with corresponding transition rates, build the midpoint of the power model and can be expressed as a Markov chain as shown in Fig.2. Modeling the idle time between two uplink transmissions as a negative exponential distributed function with mean $1/\lambda$ leads to the leaving transitions from Idle state with the rate λ. The particular rates λ_i are the result of weighting λ with individual power state probabilities ϑ_i:

$$\lambda_i = \vartheta_i \cdot \lambda \qquad \text{for } i \in \{2, 3, 4\}, \tag{1}$$

$$\sum_{i=2}^{4} \vartheta_i = 1. \tag{2}$$

They reflect the probability that the device must transmit at a specific transmission power to achieve the required Signal to Noise Ratio (SNR) at the addressed base station under the given radio conditions. The actual values of ϑ_i depends on the cell environment, e.g., urban or rural area, the UE's mobility, e.g., pedestrian or vehicular movement, and finally the utilized carrier frequency. In this paper, and according to [6], ϑ_i is derived from ray tracing simulations and channel emulations of three environments, three mobility patterns, and two common carrier frequencies as listed in Tab. I.

The time spent in any active state $1/\mu_{\mathrm{UL},i}$ is derived from the channel dependent uplink throughput in each state $R_{\mathrm{UL},i}$ and the average upload file size D_{UL}:

$$\mu_{\mathrm{UL},i} = \frac{R_i}{D_{\mathrm{UL}}} \qquad \text{for } i \in \{2, 3, 4\}. \tag{3}$$

Especially in the Max state, where the maximum transmission power is limited to 23 dBm [9] and the UE must fall back to more robust Modulation and Coding Scheme (MCS), $R_{\mathrm{UL},4}$ may be significantly lower than in the other modes. The model considers this rate degradation according to empirical studies performed in [10] and [11], which leads to a longer residence time in Max state.

By deriving the equilibrium equations for the Markov model in Fig. 2 and solving the linear equation system we get the state probabilities p_i with

$$p_i = \begin{cases} \frac{1}{1+\sum_{j=2}^{4}(\lambda_j/\mu_j)} & \text{for } i = 1, \\ \frac{\lambda_i/\mu_i}{1+\sum_{j=2}^{4}(\lambda_j/\mu_j)} & \text{for } i \neq 1. \end{cases} \quad (4)$$

With this state probabilities and the average power consumption in each state $\bar{P}_i$ the average long term power consumption of the UE can be expressed as

$$P_{\mathrm{Total}} = \sum_{i=1}^{4} \bar{P}_i \cdot p_i. \quad (5)$$

B. Model Extension for Downlink and Carrier Aggregation

In order to apply CoPoMo to mixed uplink/downlink transmissions and carrier aggregation the model must be extended. The necessary modifications will be explained in this subsection. A timeline of an exemplary uplink transmission according to classic CoPoMo and Fig. 2 is shown in the upper part of Fig. 3. It shows the residence time in each state according to calculated long-term state probabilities from Eq. 4. Although the model explicitly does not include transitions between two distinct transmitting states (cf. Fig. 2), those states are still grouped next to each other in the figure. This is legitimate, because the power consumption of a device is assumed to be independent of the order the states are traversed. Therefore, only the average time spent in each state must be maintained.

To extend the power model for downlink transmissions the following assumptions were made:

- The data rates of the uplink R_{UL} and the downlink R_{DL} are affected by the radio channel in the same way. Therefore, the relation between the two rates r_{DLUL} is fixed to $r_{\mathrm{DLUL}} = R_{\mathrm{UL}}/R_{\mathrm{DL}}$.
- Realistic downlink transmissions typically contain a fraction of uplink data, e.g. requests and acknowledgments. The relation of downlink data size D_{DL} and uplink data size D_{UL} is described by $d_{\mathrm{DLUL}} = D_{\mathrm{UL}}/D_{\mathrm{DL}}$.
- The arrangement of uplink transmissions during an ongoing download has no effect on the power consumption. It is assumed, that no additional time is spent in tail states [3].
- Downloading data during an active uplink transmission does not increase the average power consumption of the device in the current active state.
- The power consumption during a pure downlink transmission $\bar{P}_{\mathrm{DL}}$ (without any uplink) equals to the power consumption in Low mode as shown in previous studies [3]. Therefore, $\bar{P}_{\mathrm{DL}} = \bar{P}_2$.

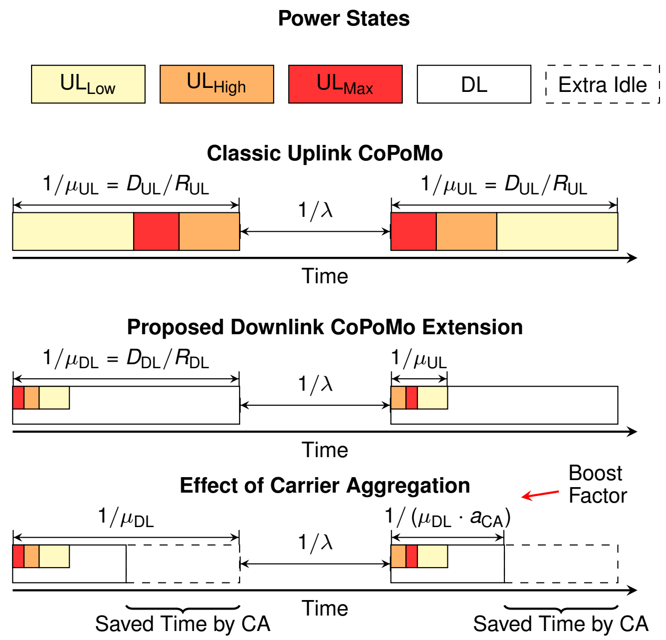

Fig. 3. Comparison of Uplink CoPoMo and the Proposed Extension for Downlink and Carrier Aggregation

- Carrier aggregation will be modeled as a boost factor $a_{\mathrm{CA}} \geq 1$ that increases the downlink data rate R_{DL}. As measurements in Sec. IV will show, enabling an additional Component Carrier (CC) leads to a constantly higher power consumption in all active states.

With these assumptions a downlink transmission without CA ($a_{\mathrm{CA}} = 1$) can be arranged in a time line as shown in the middle of Fig. 3. The example shows two downlink transmissions (white) with an associated uplink portion (yellow, orange and red) arranged to the beginning of each block. By using μ_{DL} instead of μ_{UL} to calculate the stationary distribution of the Markov chain (Eq. 4), the resulting state probabilities reflect the relative stay time of each mode as if the device was continuously uploading during the entire downlink transmission period of

$$\frac{1}{\mu_{\mathrm{DL}}} = \frac{D_{\mathrm{DL}}}{R_{\mathrm{DL}}} = \frac{D_{\mathrm{UL}} \cdot r_{\mathrm{DLUL}}}{R_{\mathrm{UL}} \cdot d_{\mathrm{DLUL}}}. \quad (6)$$

As the actual uplink time during the particular power states is only $1/\mu_{\mathrm{UL}}$, the remaining time consists of pure downlink traffic consuming $\bar{P}_{\mathrm{DL}}$.

When enabling an additional CC and therefore increasing the downlink data rate by $a_{\mathrm{CA}} > 1$ this will result in a shorter downlink transmission time as shown in the bottom row of Fig. 3. During this saved time the UE immediately enters the Idle state, thus saves energy.

Let $t_i = 1/\mu_{\mathrm{DL},i}$ the average time spent in a particular state i without CA and $t_{\mathrm{ULDL},i} = 1/(\mu_{\mathrm{DL},i} \cdot a_{\mathrm{CA}})$ the actual active time with CA then the extra idle time gained by CA is

$$t_{\mathrm{idle},i} = t_i - t_{\mathrm{ULDL},i}. \quad (7)$$

The average uplink time is derived from its data size and rate $t_{\mathrm{UL},i} = D_{\mathrm{UL}}/R_{\mathrm{UL},i}$ and the remaining active time consists of

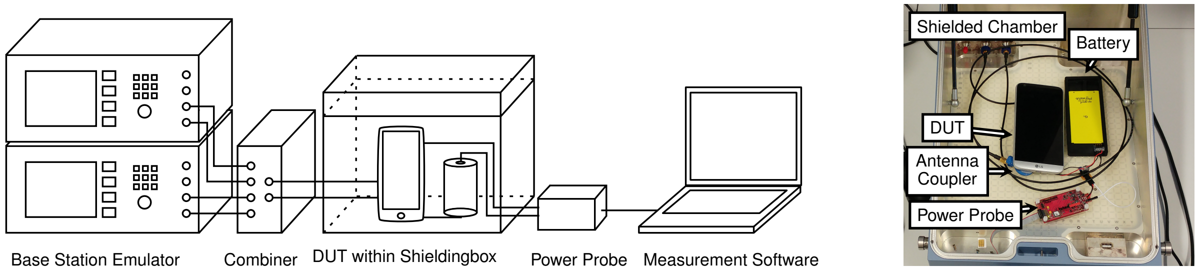

Fig. 4. Schematic Overview of the Measurement Setup and Photography of the Measurement Setup Inside a Shielded Chamber

only pure downlink transmissions:

$$t_{\mathrm{DL},i} \quad = \quad t_{\mathrm{ULDL},i} - t_{\mathrm{UL},i} \qquad \text{for } t_{\mathrm{ULDL},i} > t_{\mathrm{UL},i}. \quad (8)$$

Cases where the uplink transmission time is larger than or equal to the downlink activity time are covered by the classic CoPoMo, thus are not further discussed in this paper.

According to the calculated time intervals, the mixed power consumption $\tilde{P}_i$ can be described as

$$\tilde{P}_i = \frac{t_{\mathrm{UL},i}}{t_i}\bar{P}_i + \frac{t_{\mathrm{DL},i}}{t_i}\bar{P}_{\mathrm{DL}} + \frac{t_{\mathrm{idle},i}}{t_i}\bar{P}_1 \quad \text{for } i \in \{2,3,4\} \quad (9)$$

and $\tilde{P}_1 = \bar{P}_1$. This model now allows a simulative rating of the impact of CA on the UE power consumption pursuant to different system and context parameters.

IV. Measurements

In order to fed the proposed power consumption model with appropriate values and to analyze the static power consumption caused by downlink CA in today's UE, we performed excessive measurements with two Common-off-the-shelf LTE Device Under Test (DUT) in a laboratory environment, abbreviated as DUT-A and DUT-B:

- DUT-A: LG G5
- DUT-B: Samsung Galaxy S5 Neo

A. Measurement Setup

A measurement setup, as outlined in Fig. 4, was built to create a fully controlled environment consisting of an LTE Base Station Emulator (BSE), an LTE UE, and measurement equipment to determine the UE power consumption. The BSE was a composite of two *Rohde & Schwarz CMW500* that allows the emulation of an LTE cell with up to three CCs à 20 MHz at arbitrary frequencies and using 2×2 Multiple Input Multiple Output (MIMO) on each carrier. Due to limitations of the available DUT, measurements with CA were limited to the Primary Carrier Component (PCC) (the actual serving cell) and a single Secondary Carrier Component (SCC) which formed the aggregated part. The signal was fed into a shielded chamber as shown in Fig. 4 to avoid interference with public networks. In order to measure the power consumption of the DUT, the battery has been extracted and replaced by wired dummy which was interconnected with a measurement probe. The power consumption was captured by a *Hitex Powerscale* with a sampling rate of 100 kHz and evaluated on a computer.

If not stated otherwise the measurements were performed in Single Input Single Output (SISO) configuration at bandwidths of 10 MHz for each CC. During an active connection the UE continuously got full RB allocations on all active CC forcing the UE to decode random padding bits and withdraw them in downlink direction and to fill padding bits in the uplink. By doing so, no user-space application was required on the DUT to generate traffic. This minimized the influence of other power consuming components (e.g. CPU, memory, display) on measurements of the LTE part, as only the over-all power consumption of the DUT could be measured.

B. Band Specific Power Consumption

The first measurement targets the question whether it makes a difference in terms of power consumption if a UE receives the PCC and SCC in specific bands and if there are any differences between intra-band and inter-band carrier aggregation. To quantify this, we sequentially connected the two DUT to a serving cell in one of three different bands which are licensed for LTE in Germany: Band 3 (1800 MHz), Band 7 (2600 MHz), and Band 20 (800 MHz). Subsequently, SCC at the listed frequencies has been added covering all possible permutations with two carriers and three bands. The additional power consumption in relation to single carrier operation is plotted in Fig. 5 for both DUT.

It can be seen, that depending on the selected permutation the additional power consumption of both devices is between 190 mW and 403 mW and varies in the order of 100 mW for a single device. Particularly, intra-band CA leads to the smallest power increase with two exceptions: First, DUT-A does not support any intra-band CA in the 800 MHz band. Second, for DUT-B the combination of 2600 MHz and 1800 MHz consumes slightly less power than the corresponding intra-band constellation at 2600 MHz. For both DUT with the exclusion of intra-band CA, enabling an SCC in the 2600 MHz band results in the highest power draw compared to the other covered bands.

C. Number of Resource Blocks vs. Power Consumption

The second measurement aims at the cause of the power draw increase, whether it is caused by the increased decoding effort or by powering an additional receive chain. For this purpose we performed two power measurement series for various numbers of allocated RBs with both, PCC and SCC, in the 2600 MHz band at 20 MHz bandwidth. This allows a total downlink allocation of maximum 200 RBs at the same time. The first series allocates sequentially 8 to 100 RBs on the PCC only. Afterwards SCC is being added and the sequence is appended to 200 RBs. The second series covers the same range but enables the SCC right from the beginning and shares the allocated RBs equally among the two CC. Fig. 6 shows the results of these measurements for DUT-A

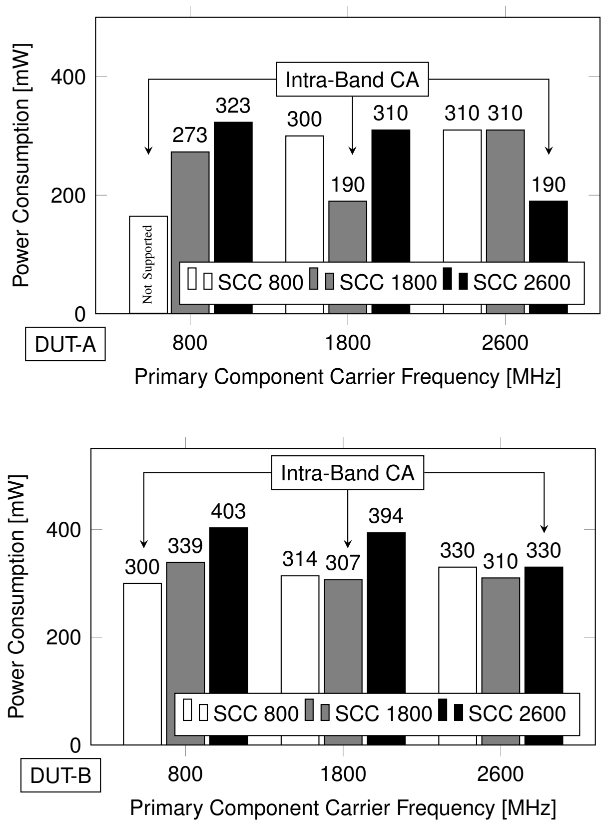

Fig. 5. Additional Power Consumption for Carrier Aggregation at Different Frequencies for DUT-A and DUT-B

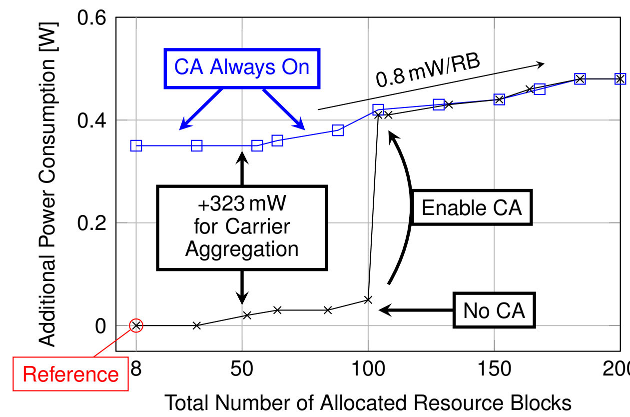

Fig. 6. Normalized Power Consumption of DUT-A in Relation to the Number of Allocated Resource Blocks and Carrier Aggregation

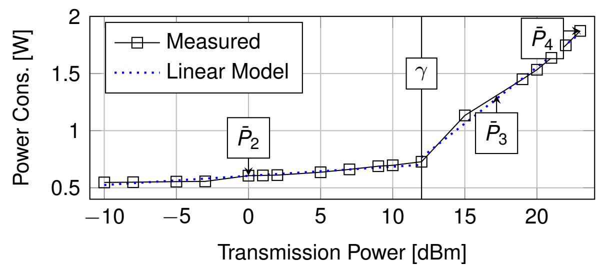

Fig. 7. Power Consumption of DUT-B at 800 MHz in Relation to Transmission Power.

TABLE II
EMPIRICAL MODEL PARAMETERS FOR POWER AMPLIFIER MODES

Parameter	DUT-A		DUT-B	
Frequency [MHz]	800	2600	800	2600
$\bar{P}_1$ [mW]	97	97	30	30
$\bar{P}_2$ [mW]	753	860	604	980
$\bar{P}_3$ [mW]	1912	1578	1309	1515
$\bar{P}_4$ [mW]	3053	2450	1873	1993
γ [dBm]	15	10	12	12

normalized to the PCC-only consumption at 8 RBs. While the power consumption linearly grows with an approximated rate of 0.8 mW per RB, adding the SCC constantly causes a jump of 323 mW independent of the decoding complexity. As soon as multiple carriers are activated, the distribution of allocated RBs among the carriers makes no difference in the power consumption. At this place it must be noted that in contrast to Fig. 5 the operating bandwidth now is twice as high as before, thus the additional power consumption for CA has roughly doubled as well. Based on this knowledge, the base station should always prefer – if possible without the loss of service quality – a single carrier allocation over an aggregated allocation as long as the number of RBs fits into the PCC. Due to space restrictions the results for DUT-B are omitted as it behaves similarly to DUT-A.

D. Uplink Power Consumption

As mentioned in Sec. III the highest power draw of LTE equipment is caused by the uplink. Although the focus of this paper lies on the analysis of the downlink, realistic usage patterns of LTE devices always contain a certain fraction of uplink traffic. Consequently, a simulation of the over-all power consumption of a UE requires power measurements in the distinct power states (cf. Fig. 2). Since the uplink consumption has been examined in previous works [12], only a brief overview of our results is given. Measurements were made for both DUT at 800 MHz and 2600 MHz with a bandwidth of 10 MHz at full RB allocation. The UE transmission power was set by the BSE covering the range of −10 dBm to 23 dBm while capturing the power draw of the DUT. As an example the measurement results for DUT-B at 800 MHz are given in Fig. 7. For the power model the consumption is approximated by two linear graphs. These were separated by the breakpoint γ which marks the switching point from a low power amplifier to a high power amplifier within the device [3]. While the power consumptions of the Idle state $\bar{P}_1$ and the Max state $\bar{P}_4$ are clear, the representative consumption for Low mode $\bar{P}_2$ is taken at 0 dBm and for $\bar{P}_3$ (High) at $(\gamma+23)/2$ dBm [3], [12]. The determined values for both DUT are listed in Tab. II.

V. SIMULATIONS

Based on measurements in Sec. IV, which we fed into the proposed power consumption model (cf. Sec. III-B), we performed simulations to evaluate the power-savings potential of CA in various scenarios. If not stated otherwise the simulations are configured as listed in Tab. III.

A. Impact of Data Size

The first simulation varies the average download file size D_{DL} for both DUT at 800 MHz and 2600 MHz as shown in

TABLE III
DEFAULT SETTINGS FOR SIMULATIONS

Parameter	Value
Frequency	800 MHz, 2600 MHz
Bandwidth PCC, SCC	10 MHz each
CA Type	Intra-Band-CA
CA Boost Factor a_{CA}	2
Antenna Configuration	SISO
Environment	Suburban
Channel Model	AWGN
Arrival Rate λ	$1/(5\,\mathrm{min})$
File Size D_{DL}	1 Gbit
Transmission Protocol	TCP
UL/DL Ratio d_{DLUL}	0.02
UL/DL Rate Ratio r_{DLUL}	0.5

Fig. 8. At small amounts of data ($D_{DL} < 2\,\mathrm{Mbit}$) most of the power consumption is issued by the idle state, thus being independent of frequency and aggregation type. For larger transmissions raises the 2600 MHz curve much earlier to a higher power level than the curve of the lower band. This is mainly caused by the uplink fraction of the transmission and the increased attenuation in this band, which requires in average a higher transmission power of the UE. Since both devices consume more power during pure data reception at higher frequencies (cf. $\bar{P}_2$ in Tab. II), CA is especially beneficial as the expensive active time is shortened by the boosted data rate and consequently allows the device to fall back quickly into Idle state. Both devices consume at this band and at a mean file size of 1 Gbit about 30 % less power if CA is added. Changing the frequency to 800 MHz results in savings of at least 21 % to 26 % depending on the device.

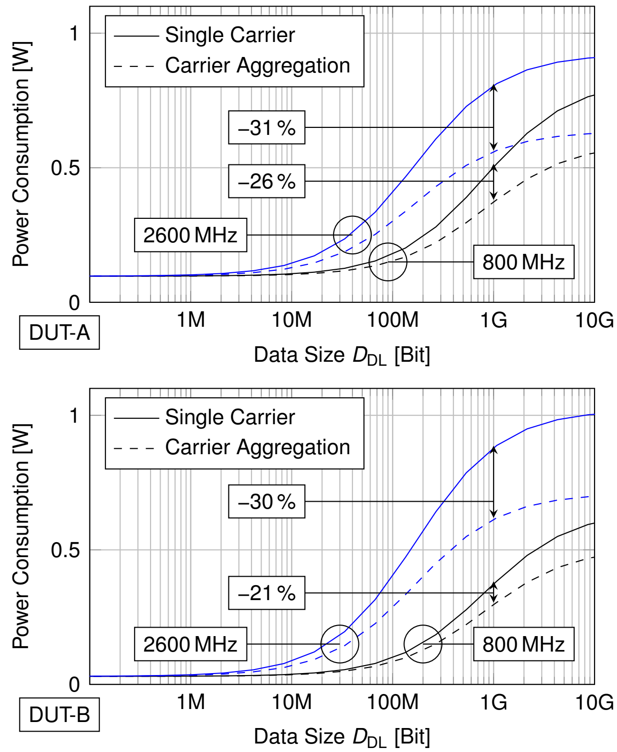

Fig. 8. Power Consumption of DUT-A and DUT-B in Relation to Average Transmission File Size (cf. Tab. III)

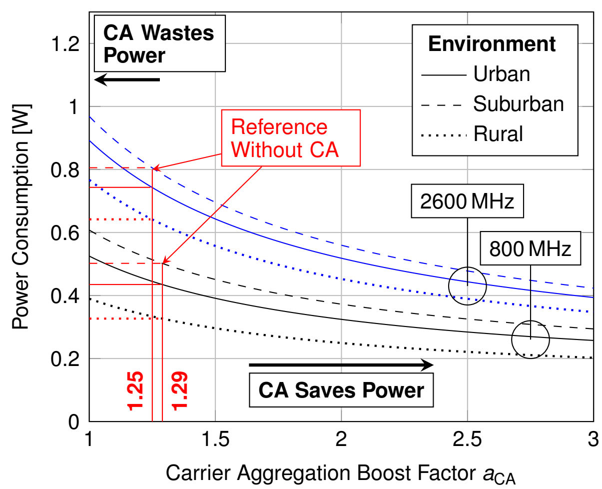

Fig. 9. Power Consumption of DUT-A in Relation to Carrier Aggregation Boost Factor for Different Cell Environments

B. Impact of Cell Environment and Boost Factor

To analyze the impact of the cell environment on the UE power draw, simulations at urban, suburban, and rural building densities were performed. In addition, the CA boost factor a_{CA} was varied to identify the point from which CA outperforms the single CC consumption. The results for DUT-A can be seen in Fig. 9. Results of DUT-B are omitted due space limitations and similar behavior. As reference, the power consumption of particular scenarios without CA are drawn in red until they intersect with their corresponding CA curve. It can be seen, that the total power consumption of a UE varies with the chosen environment. Rural environments issue the lowest power consumption due to the high probability for line-of-sight connections. The highest consumption takes place in the suburban case as the inter-site distance is still very high (cf. Tab. I) but a large fraction of the covered area has no line-of-sight connection, hence the signals suffers of increased attenuation. In the urban case the reduced cell size decreases the probability for high power states.

Furthermore, the results show that the intersection of power consumption with CA and without CA happens at exactly the same boost factor a_{CA} regardless of the chosen environment. Instead, it depends on the device and operating frequency and lies in a range of 1.25 to 1.29 for DUT-A. This means, that CA reduces the power consumption of an UE if it increases the downlink data rate at least by an order of 25 % to 29 %. In general, at higher frequencies smaller boost factors are required to reduce the power draw of the device. While higher boost factors lead to further power savings, the savings do not scale linearly with the boost factor, but rather stagnate beyond values of 2 to 3. In any case, a higher boost factor leads to larger power savings of the UE.

C. Impact of Mobility and Boost Factor

After analyzing relationship of CA and the building density on the power demands of LTE equipment, now the impact of mobility will be investigated. Mobility affects the radio channel in terms of fast fading, which is basically a result of the signal's multipath propagation that leads to constructive

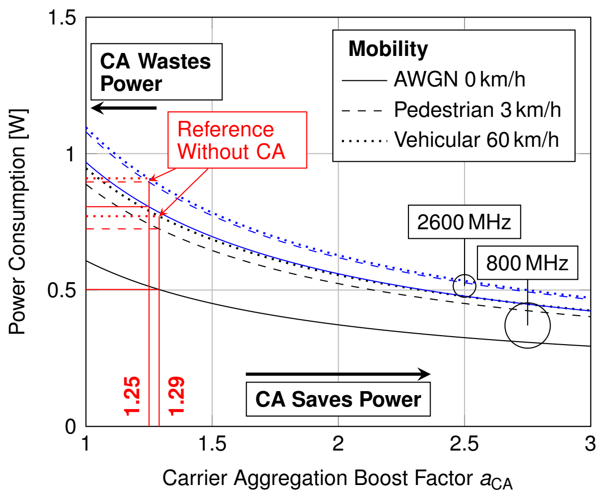

Fig. 10. Power Consumption of DUT-A in Relation to Carrier Aggregation Boost Factor for Different Mobility Patterns

or destructive interference of the distinct signal paths at the receiver. As this effect highly depends on position and frequency, the signal fluctuates more intensively if sender or receiver move faster. Consequently, this reduces the throughput in both directions and requires the UE to spend more time in active transmission modes. Fig. 10 shows the simulated average power consumption of DUT-A for two frequency bands, three mobility types and CA boost factors from 1 to 3. Again, DUT-B behaves similarly, hence the results are omitted due to limited space. It can be seen, that mobility – especially in the 800 MHz band – significantly increases the power demands of DUT-A if compared to the static AWGN case in average by 41 %. Conversely, increasing the speed of movements from 3 km/h to 60 km/h increases the power draw in average only by 6 % at 800 MHz; at 2600 MHz the power increase is even negligible at 1 %.

The intersection point of power consumption with CA and without CA is located at the exactly same boost factor for a given frequency and device independent of the mobility and do not differ from the previous simulation. This makes CA beneficial for the battery lifetime of mobile equipment in any case, no matter of the velocity and building density as long as the achieved boost in data rate overbalances the increased CA power draw.

VI. Conclusion

The results of this paper show that Carrier Aggregation (CA) is beneficial for the power consumption of LTE devices when used deliberately. Measurements of existing LTE-A devices showed that the use of multiple Component Carrier (CC) entails an increased power draw for supplying additional receive chains in the order of 300 mW. Therefore, as long as the allocated number of Resource Blocks (RBs) fits into a single CC, CA should be avoided since this only leads to an increased power draw. This device-specific power increase varies with the chosen band. In most cases inter-band CA pointed out a slightly higher power draw than intra-band CA.

Applying the empirical data into a proposed downlink extension of the Context-Aware Power Consumption Model (CoPoMo) allowed a quantitative evaluation of the costs and benefits of CA for different mobility patterns, environments and frequencies. The simulations show, that CA has a positive effect on the power consumption, if it boosts the downlink data rate by at least 25 % to 29 %. At this point the power savings by additional idle time compensate the higher power draw during an active transmission. The exact values depend on the carrier frequency of the primary carrier but not on the building density or whether the UE is static or moving quickly with a vehicle.

Further simulations showed increasing power savings as the average file size of downloads grows. In the simulated scenario at a mean file size of 1 Gbit, which is typical for multimedia videos or navigation map data, a power reduction of 21 % to 31 % can be achieved by CA.

Acknowledgment

Part of the work on this paper has been supported by Deutsche Forschungsgemeinschaft (DFG) within the Collaborative Research Center SFB 876 "Providing Information by Resource-Constrained Analysis", project A4.

References

[1] A. R. Jensen, M. Lauridsen, P. Mogensen, T. B. Sørensen, and P. Jensen, "LTE UE power consumption model: For system level energy and performance optimization," in *Vehicular Technology Conference (VTC Fall), 2012 IEEE*, September 2012, pp. 1–5.

[2] M. Lauridsen, L. Noël, T. B. Sørensen, and P. Mogensen, "An empirical LTE smartphone power model with a view to energy efficiency evolution," *Intel Technology Journal*, vol. 18, no. 1, pp. 172–193, 2014.

[3] B. Dusza, "Context aware power consumption modeling for energy efficient mobile communication services," Ph.D. dissertation, TU Dortmund, December 2013.

[4] R. Sanchez-Mejias, Y. Guo, M. Lauridsen, P. Mogensen, and L. A. M. R. de Temino, "Current consumption measurements with a carrier aggregation smartphone," in *2014 IEEE 80th Vehicular Technology Conference (VTC2014-Fall)*, September 2014, pp. 1–5.

[5] L. A. Sonkusare and S. N. Dhage, "LTE UE performance evaluation for carrier aggregation and voice-over-LTE," in *2015 International Conference on Applied and Theoretical Computing and Communication Technology (iCATccT)*, October 2015, pp. 642–647.

[6] B. Dusza, C. Ide, L. Cheng, and C. Wietfeld, "CoPoMo: A context-aware power consumption model for LTE user equipment," *Transactions on Emerging Telecommunications Technologies (ETT), Wiley*, vol. 24, no. 6, pp. 615–632, October 2013.

[7] B. Dusza, P. Marwedel, O. Spinczyk, and C. Wietfeld, "A context-aware battery lifetime model for carrier aggregation enabled LTE-A systems," in *2014 IEEE 11th Consumer Communications and Networking Conference (CCNC)*, January 2014, pp. 13–19.

[8] *3GPP TR 25.813 - Physical layer aspects for evolved Universal Terrestrial Radio Access (UTRA)*, 3rd Generation Partnership Project Technical Report, Rev. V7.1.0, September 2006.

[9] *3GPP TS 36.101 - Technical Specification Group Radio Access Network; Evolved Universal Terrestrial Radio Access (E-UTRA); User Equipment (UE) radio transmission and reception (Release 12)*, 3rd Generation Partnership Project Technical Specification, Rev. V12.7.0, March 2015. [Online]. Available: http://www.3gpp.org/ftp/specs/archive/36_series/36.101/

[10] B. Dusza, C. Ide, and C. Wietfeld, "Measuring the impact of the mobile radio channel on the energy efficiency of LTE user equipments," in *Proc. of the 21st International Conference on Computer Communication Networks (ICCCN), 2nd International Workshop on Context-aware QoS Provisioning and Management for Emerging Networks, Applications and Services (ContextQoS)*. Munich, Germany: IEEE, July 2012.

[11] B. Dusza, C. Ide, P. B. Bök, and C. Wietfeld, "Optimized cross-layer protocol choices for LTE in high-speed vehicular environments," in *2013 9th International Wireless Communications and Mobile Computing Conference (IWCMC)*, July 2013, pp. 1046–1051.

[12] B. Dusza, C. Ide, L. Cheng, and C. Wietfeld, "An accurate measurement-based power consumption model for LTE uplink transmissions," in *2013 IEEE Conference on Computer Communications Workshops (INFOCOM WKSHPS)*, April 2013, pp. 49–50.